

Laboratory fatigue assessment of large geocomposite-reinforced double-layered asphalt concrete beams

P. Jaskula, D. Rys, M. Stienss & C. Szydlowski

Faculty of Civil and Environmental Engineering, Gdansk University of Technology, Gdansk, Poland

M. Golos

Tensar International Limited, Blackburn, Lancashire, UK

J. Kawalec

Faculty of Civil Engineering, Silesian University of Technology, Gliwice, Poland

Tensar International s.r.o., Cesky Tesin, Czech Republic

ABSTRACT: Geosynthetic reinforcement of asphalt layers has been used for several decades. Evaluation of the influence of these materials on pavement fatigue life is still ongoing, especially for new types of geocomposites. This paper presents the evaluation of fatigue performance of large asphalt concrete beams reinforced with a new type of composite in which square or hexagonal polypropylene stiff monolithic paving grid with integral junctions is bonded to polypropylene non-woven paving fabric. Unreinforced samples were used as reference. Fatigue testing was performed in the scheme of four-point bending test (4PB-PR) in the controlled strain mode at +13°C. Test results were analysed in several aspects, including the standardised approach based on stiffness reduction, but also using critical strain at one million cycles. A new parameter – relative increase in fatigue life – was introduced in the analysis as well. On the basis of the obtained results, it can be concluded that the evaluated composites will have evident positive effect on pavement performance and may contribute to a several fold increase in fatigue life of pavement structure. More benefits in terms of pavement bearing capacity are expected in the case of reinforcement of thick and new asphalt pavements. The use of hexagonal geogrid resulted in greater improvement of fatigue resistance than composites with square geogrid.

Keywords: grid reinforcement, fatigue of asphalt pavements, four-point bending test, crack propagation, reflective cracking

1 INTRODUCTION

Reinforcement of asphalt pavements with geocomposites improves bearing capacity effectively, as proved in numerous previous studies (Brown, 1985; Correia, 2014; Graziani et al., 2014). The benefits are notably visible when geocomposites are used in rehabilitation of old, cracked pavement sections (Canestrari et al., 2013; Pasquini et al., 2013; Zieliński, 2013). However benefits are clearly observed in the field (Al-Qadi, 2006; Ragni et al., 2020; Spadoni et al., 2021), the literature still lacks a detailed description (Solatiyan et al., 2020) of the quantified contribution of geocomposite reinforcement to an increase in bearing capacity or reduction of crack propagation of asphalt pavements. Importantly, geocomposites are installed on

top of an existing pavement during placement of new layers and provide different functions according to the type of geosynthetic used (Nguyen et al., 2021; Shukla & Yin, 2004).

The main objective of the presented studies was to evaluate the probable contribution of the new type of geocomposite to extension of bearing capacity, reduction of crack propagation and overall fatigue life extension of asphalt pavement. The evaluation was conducted on the basis of laboratory fatigue tests of double-layered asphalt specimens in four-point bending scheme.

2 METHODOLOGY

2.1 *Experiment planning*

It is expected that reinforcement of asphalt layers with grid geocomposites should increase the fatigue life and delay crack propagation in asphalt pavements. Therefore, double-layer asphalt mixture systems were subjected to cyclic loading in order to determine their fatigue performance. Reference systems consisted of two layers of asphalt concrete, AC 11 W for the lower layer and AC 16 W for the upper layer, bonded with tack coat (Jaskula et al., 2021). Reinforced systems were prepared using same asphalt concrete mix design; the only differences consisted in the implementation of geogrid reinforcement at layer interface and application of a higher quantity of asphalt emulsion used for tack coat. Results obtained for reinforced systems were compared to results obtained for reference system in order to obtain the relative increase in fatigue life. Two groups of specimens were considered: plain and with notch. The idea of testing plain specimens was to simulate the effect of reinforcement in a new pavement structure, where geocomposite may contribute to transfer of tensile stresses and delay crack formation. Notched systems were tested in order to simulate the effects of reinforcement in a rehabilitated pavement, where cracks have already formed in the lower layer and geocomposite prevents reflecting cracking.

2.2 *Laboratory testing in 4PB scheme*

Fatigue testing was performed in the scheme of four-point bending test on prismatic specimens (4PB-PR). A novel aspect of the approach was the use of significantly larger beams consisting of two layers of asphalt mixture with composite reinforcement and emulsion tack coat at their interface. Since such tests may be significantly affected by the size effect, the specimens were larger than those used in typical procedures of fatigue testing with the 4PB-PR scheme. The adopted width of the sample (170 mm) was based on the assumption that the width of the geogrid placed between asphalt layers in the sample must include at least 2 full pitches (both square and hexagon) of geogrid. The distance between axes of the end supports equalled 740 mm. The distance between axes of the loading supports equalled 247 mm. Due to load set-up (bottom loading actuator) of the testing equipment, the specimens had to be placed in clamps of the testing machine in an inverted position in comparison to their natural arrangement in the pavement (i.e., the 30 mm of the lower AC 11W asphalt mixture and the reinforcement grid facing upwards). The loading actuator bent the beam upwards, so the location of the compression and tension zones within the specimen reflected real conditions. The test was performed in a climatic chamber at a constant temperature of +13 °C, which is the equivalent temperature adopted in the design of flexible pavements in Poland (Judycki et al., 2017; Pszczola, 2019). A view of the test equipment with marked dimensions of specimen and frame is presented in Figure 1.

Beams were subjected to cyclic loading that caused a sinusoidal change in strain from 0 to the pre-set maximum value. The following maximum strain values were adopted: 400, 500, 600, 700 and 800 μ strain. For each strain level and for a given type of reinforcement, a single specimen was tested. Bending was forced only in one direction, so that the grid would function in the zone subjected to tension, like in a full-scale pavement structure. The loading frequency equalled 1 Hz. The maximum number of loading cycles equalled 300,000, which resulted in the maximum testing time of 84 hours per test.



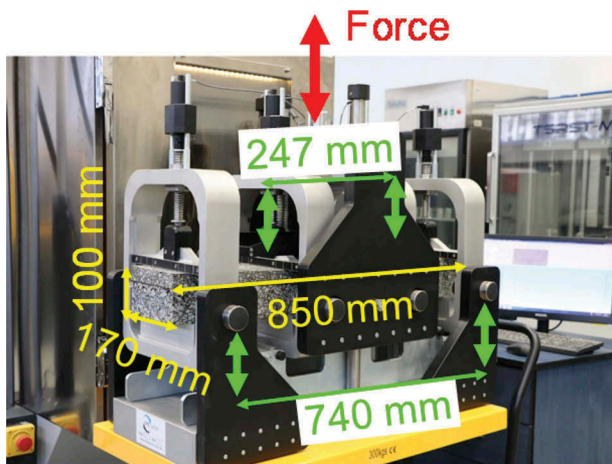


Figure 1. 4PB Equipment used for laboratory testing of double-layer specimens.

2.3 Methodology of analysis of the test results

During the fatigue testing of asphalt mixtures in the controlled pre-set strain mode, the consecutive cycles result in a gradual decrease in the stiffness modulus (and, therefore, the stress induced in the specimen), which is indicated by the continuous decrease in the force needed to induce the adopted strain level. The obtained results were analysed in terms of the initial stiffness, the number of cycles to failure, fatigue curves, strain at one million load cycles and relative increase in fatigue life. A detailed description of the parameters is given below.

Pre-set tensile strain [-]: maximum strain of the extreme tension fibres of the cross section, in the case of homogenous isotropic material. In the performed fatigue tests with controlled strain mode this value is constant for the duration of the entire test. The value of tensile strain is calculated on the basis of vertical deflection measured at the centre of the beam by a LVDT sensor. In fact, the value of ε_t is a theoretical value, since beams are not homogenous and consist of two asphalt layers with various values of stiffness modulus. Moreover, partial slippage occurs at the interface between two layers. Therefore, the strain was defined in this study as “pre-set”, which means that it is the value set in the UTM software and real value of tensile strain differs from the pre-set value.

$$\varepsilon_t = 12 \frac{\delta \cdot h \cdot 10^6}{3S_w^2 - 4L_w^2} \quad (1)$$

where:

ε_t : peak pre-set tensile strain, constant value for the duration of the entire test,

δ : vertical peak deflection at the centre of the beam [mm],

h : beam height (100 mm),

S_w : support span width (740 mm),

L_w : loading span width (247 mm).

Stiffness S [MPa]: equivalent to the stiffness modulus of the system in a given loading cycle in the test. Stiffness in any given cycle may be calculated from (2). This parameter was excluded from the analysis in the first cycles of test due to the rapid decrease in stiffness under loading during the first stage of the test. In the presented research, the initial stiffness S_{ini} was calculated using the data from the 100th cycle.

$$S_i = \frac{\sigma_i}{\varepsilon_i} \quad (2)$$

where:

S_i : stiffness in the i -th cycle of the test,

σ_i : maximum tensile stress in the i -th cycle.

Fatigue life N_f [-]: number of cycles to fatigue failure of the specimen. Different approaches are used regarding the limit of fatigue life. The most popular definition of fatigue failure, which was also assumed in these studies, is the moment at which the stiffness S_i decreases to 50% of the initial stiffness S_{ini} .

Fatigue curve: determined by the N_f fatigue life results obtained at various strain levels. The curve enables the evaluation of the system's fatigue life at any given strain level, even outside of the tested range. The general form equation of the curve is as follows:

$$\varepsilon_i = A(N_f)^b \quad (3)$$

where:

ε_i : pre-set tensile strain,

A : slope of the fatigue curve,

b : coefficient based on the obtained fatigue test results,

N_f : fatigue life of the system.

Strain at one million load cycles ε_6 : parameter based on the fatigue curve, equivalent to the strain level at which the system's fatigue life equals one million load cycles (Corté & Goux, 1996). This parameter is used for characterisation of asphalt mixtures in terms of fatigue resistance. Higher ε_6 strain level indicates better fatigue performance of the mixture (or the entire tested layered system).

Relative increase in fatigue life RI [%]: function delivered from equation (3), expressing the increase in fatigue life of the reinforced systems in comparison to the reference systems at a given tensile strain. The formula (4) was used to calculate the values of RI.

$$RI = \frac{N_{f,mod}}{N_{f,ref}} = A_{ref}^{\frac{-1}{b_{ref}}} A_{mod}^{\frac{1}{b_{mod}}} (\varepsilon_i)^{\frac{b_{mod}}{b_{ref}}} \quad (4)$$

where:

RI: relative increase in fatigue life,

$N_{f,mod}$: fatigue life of the system reinforced with a given type of geogrid,

$N_{f,ref}$: fatigue life of the reference system,

A_{ref}, b_{ref} : coefficients obtained from the fatigue curve of the reference system,

A_{mod}, b_{mod} : coefficients obtained from the fatigue curve of the geogrid-reinforced systems,

ε_i : tensile strain.

3 MATERIALS AND SPECIMEN PREPARATION

Tests were performed on double-layered specimens prepared in the following scheme:

- bottom layer made of asphalt concrete AC 11 W 35/50 for levelling courses,
- upper layer made of asphalt concrete AC 16 W 35/50 for binder courses.

Asphalt concretes were designed and produced at the Road Research Laboratory of the Gdansk University of Technology in accordance with the EN 13108-1 standard and Polish technical guidelines WT-2:2014 for medium traffic KR3-4. The mineral mixture was composed of crushed gneiss/granite aggregate and mineral limestone filler. Effective bitumen content equalled 11.9% and 11.5% by volume, and air voids equalled 4.6% and 4.5%, in AC 11 W and AC 16 W, respectively.



Geogrid composites used in this research were produced by Tensar, Blackburn, Lancashire, UK. Two types of composite reinforcement were tested:

- composite interlayer AR-GN, i.e. square aperture geogrid bonded to non-woven fabric,
- composite interlayer AX5-GN, i.e. hexagonal geogrid bonded to non-woven fabric.

Both structural paving composites consist of two components: (1) a polypropylene stiff monolithic paving grid with integral junctions and (2) a polypropylene non-woven paving fabric. The grids used in the described composites perform the structural reinforcement function (R) of the asphalt interlayer. The tensile strength of the reinforcement was 20×20 kN/m for the square grid and 16×20 kN/m for the hexagonal grid, with a peak strain of approximately 11% in the longitudinal and transverse directions at maximum load, when tested in accordance with EN ISO 10319. The non-woven fabric used in both types of composites functions as a bonding layer during installation. Another function provided by the non-woven fabric is moisture interlayer barrier (B). The described fabric has a residual bitumen retention of approximate 1.5 kg/m^2 . Unit weight of the grid component is approximately 225 g/m^2 (square) and 210 g/m^2 (hexagonal), while the unit weight of the fabric component is 130 g/m^2 . Both composites are visible in Figure 2 (step 4).

Bitumen emulsion for surface treatments with designation C 69 B3 PU (Bitunova, Warsaw, Poland) was selected to be applied as tack coat. The emulsion was produced from 100/150 neat bitumen, whose content equalled 69%. The residual bitumen amount after emulsion decay equalled to 0.2 kg/m^2 for unreinforced systems and 1.2 kg/m^2 in case of reinforced systems. Higher content of tack coat is necessary when composite is applied, to ensure proper inter-layer bonding and stress relief function. It has to be emphasised that introducing a composite between two asphalt layers causes partial loss of inter-layer bonding, despite the higher amount of tack coat. Formation of specimens was conducted in six successive steps, which are visualised in Figure 2:

Step 1 – assembly of wooden moulds with internal dimensions of $250 \times 135 \times 1000$ mm,

Step 2 – laying and compaction of the lower asphalt layer AC 11 W, the height of layer after compaction equalled 45 mm.

Step 3 – application of tack coat of bitumen emulsion C 69 B3 PU.

Step 4 – installation of geogrid composites.

Step 5 – laying and compaction of the upper asphalt layer AC 16 W, the height of layer after compaction equalled 90 mm.

Step 6 – sawing of testing beam from the compacted specimen to the final specimen dimensions $170 \times 100 \times 850$ mm.

Step 7 – preparation of a 10 mm notch in the middle of beam length in the lower asphalt layer.

Preparation of unreinforced, reference beams was carried out in the same way, except for step 4 (installation of geogrid composites – which was omitted) and a different amount of emulsion application.

4 TEST RESULTS

The decrease in the stiffness modulus in following cycles is presented on a log-log scale in Figure 3. The results obtained for the same $600 \mu\text{strain}$ load mode were selected as an example. Figure 3 enables comparisons between the reference system without reinforcement and the systems with geogrid reinforcement, both in the case of plain and notched specimens. Typically, for specimens of single asphalt mixture, three stages of stiffness modulus decrease are distinguished: (1) initial phase, which is characterised by a rapid decrease in stiffness, mostly due to the effect of thixotropy, (2) phase of damage accumulation, when stiffness decreases gradually, (3) stage of failure, when stiffness decreases rapidly due to macro-crack formation. Reference system with plain specimen confirms these typical stages; for the specimen shown in Figure 3 the third phase begins around the 100 000th cycle. The third phase of failure was not observed for reinforced plain specimens until the 300 000th cycle.



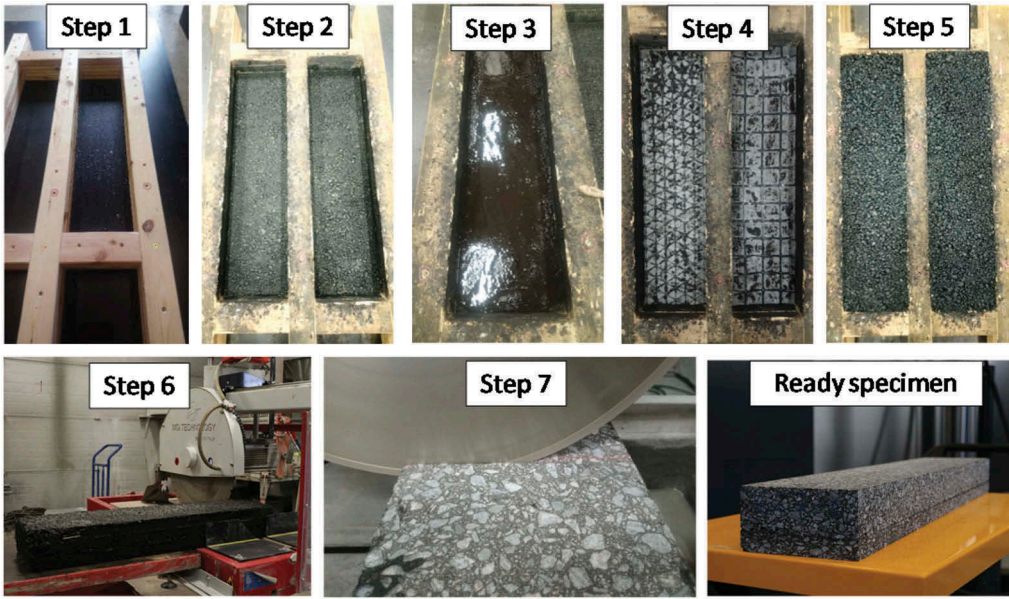


Figure 2. View of the successive steps of specimen fabrication.

In the case of all the notched systems, macro-cracks are already initiated in the lower layer. Stiffness of the reference system decreases gradually, which means that cracks penetrate from the lower layer to the upper layer. Failure of the system occurs much faster than in the case of plain specimen. In contrast, when specimen is reinforced with geogrid, the rate of decrease in stiffness is rapid at the beginning and around the 4000th cycle the rate decreases. It means that the crack propagates in the lower layer, but when it reaches the level of geocomposite reinforcement it does not pass to the upper layer. Consequently, notched systems reinforced with geocomposites remained in the second phase until the end of test (300 000 cycles). The chart presented in Figure 3 as well as visual observation of the tested specimens clearly shows that cracks did not penetrate from the lower layer to the upper layer when geocomposite reinforcement was used in the system.

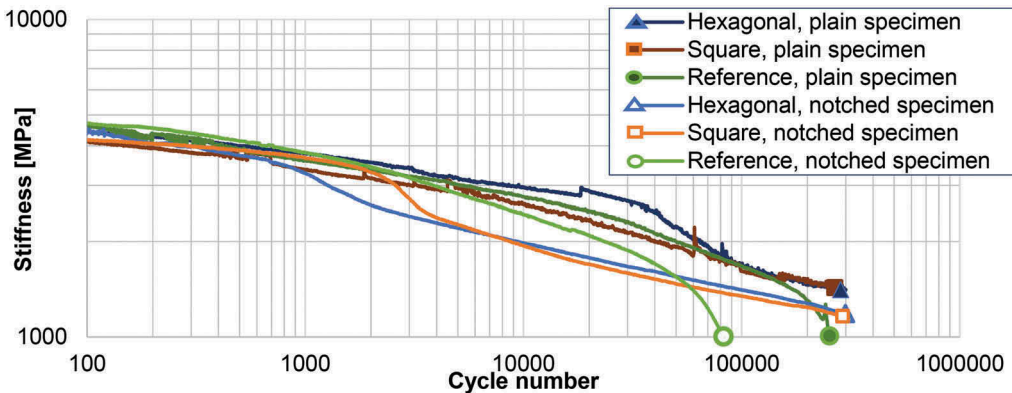


Figure 3. Comparison of the decrease in stiffness of plain and notched specimens during successive fatigue cycles at constant 600 μ strains load mode.



The results of fatigue tests expressed by the number of cycles N_f until decrease in stiffness to 50% of the initial value are presented in Figures 4 and 5 for plain and notched systems, respectively. The regression functions of fatigue curves were calculated using the least square method, and the power model (equation (3)) was used. The fatigue curve parameters A and b are given in Figures 4 and 5. They are also summarised in Table 1.

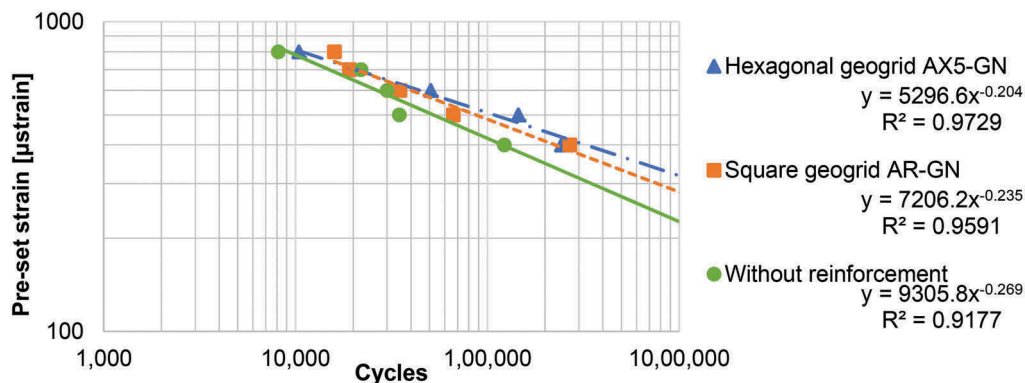


Figure 4. Fatigue model chart for double-layered asphalt beams without notch.

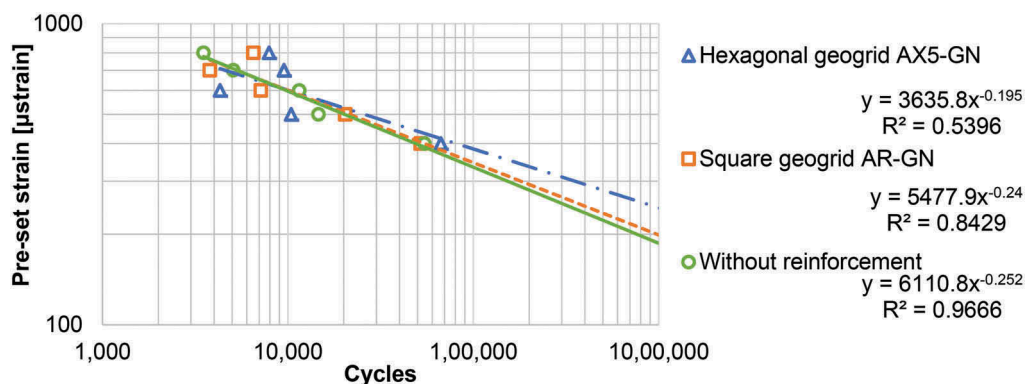


Figure 5. Fatigue model chart for double-layered asphalt beams with notch.

Table 1. Coefficients of fatigue curves.

	System	A	b
Plain specimens	Reference (without reinforcement)	9305.8	-0.269
	Reinforced with square geogrid	7206.2	-0.235
	Reinforced with hexagonal geogrid	5296.6	-0.204
Notched specimens	Reference (without reinforcement)	6110.8	-0.252
	Reinforced with square geogrid	5477.9	-0.240
	Reinforced with hexagonal geogrid	3635.8	-0.195

It was observed that at higher levels of pre-set strain fatigue life of reinforced systems was comparable to that of the reference unreinforced system. Differences are more visible at lower levels of pre-set strains, where higher fatigue life was observed for reinforced systems.

Power models fit to test results very well in the case of all the plain specimens and the reference notched system, as expressed by the high value of $R^2 > 0.9$. The fatigue life model of the notched reinforced systems does not fit the experimental data equally well. Fast crack propagation in the lower layer and delamination of two asphalt layers caused by crack propagation may be the reason of high variability in the observed values of fatigue life of the notched reinforced systems. However, a deeper analysis of the outliers visible in Figure 5 (e.g. for 600 μ strains) leads to analysis of the decrease in stiffness in subsequent load cycles (see Figure 3). The criterion of a 50% decrease in stiffness modulus was adopted for determination of fatigue life for all systems, but the process of fatigue is different in the case of non-reinforced notched system and reinforced notched systems. After failure of the lower layer, the stiffness of the whole system decreases rapidly, but then the geocomposite activates itself, which results in a lower rate of stiffness decrease, as shown in Figure 3.

The fatigue curves were used to calculate the strain at one million load cycles ϵ_6 . The results are presented in Figure 6. Higher values of ϵ_6 obtained for the reinforced systems both in the case of plain and notched systems express higher fatigue performance of those systems.

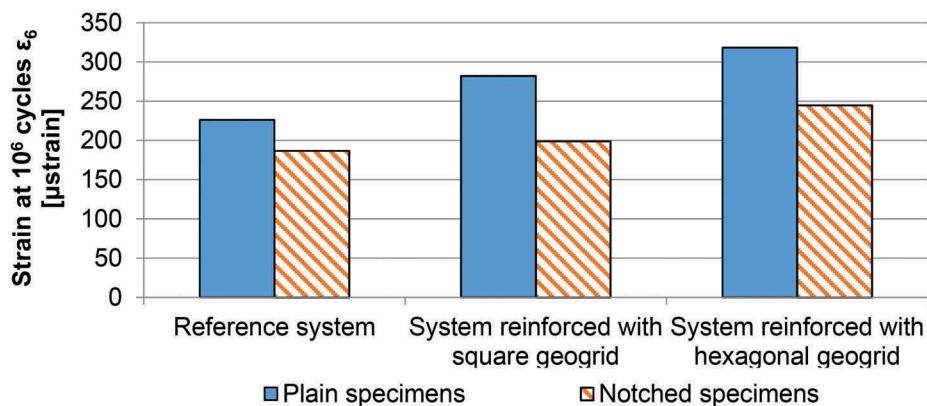


Figure 6. Critical strains at 10^6 cycles and relative change in critical strain.

5 IMPACT OF GEOCOMPOSITE REINFORCEMENT ON BEARING CAPACITY OF ASPHALT PAVEMENT

The bearing capacity of asphalt pavement is directly related to fatigue life of asphalt layers. The relative increase in fatigue life of double-layered systems was calculated according to equation (4). Coefficients A and b used in equation (3) were determined on the basis of regression coefficients summarised in Table 1. Figure 7 presents the results of relative increase in fatigue life RI for tensile strains from 80 to 200 μ strains. Plots presented in Figure 7 were developed on the basis of extrapolation of models given in Figures 4 and 5, which generates some uncertainty in the presented values. Nevertheless, it can be stated that application of hexagonal geogrids causes a severalfold increase in fatigue life. Reinforcement with square geogrids is less efficient than reinforcement with hexagonal geogrids, but it increases the fatigue life up to 4 times in comparison to the reference systems.

The assumed levels of tensile strain correspond to the values which occur at the bottom of the asphalt layers in pavement structure loaded by wheels of a heavy vehicle. Determination of tensile strain at the bottom of the asphalt layers is a complex process, as it depends on several factors. However, some general dependencies can be formulated. Tensile strain decreases when: 1) axle load decreases, 2) total thickness of the asphalt layers increases, 3) elastic modulus of the

subbase and subgrade increases, 4) stiffness of the asphalt layers increases (e.g. due to a decrease in temperature and an increase in vehicle speed). Since the experiment was performed in laboratory, fatigue life of the systems as well as the pre-set tensile strains do not correspond to the values representative for the entire pavement structure. A shift factor should be used between the fatigue life obtained for systems tested in laboratory and the fatigue life of pavement structure. It is expected that the shift factor for the reference system is around 20 (e.g. shift factor for Asphalt Institute fatigue criteria equals 18.4). The shift factor for reinforced systems is unknown. Nevertheless, the relations between the increase in fatigue life of reinforced pavements and reinforced beams tested in laboratory conditions remain the same – they are presented in Figure 7.

Figure 7 shows evidently that reinforcement of pavement with geocomposites improves its bearing capacity. Reinforcing with hexagonal geogrids is more beneficial than reinforcing with square geogrids. When reinforcement is used in plain systems, which simulate new pavements, the relative increase in fatigue life is greater than in the case of notched systems, which simulate rehabilitated pavements. More beneficial effects of pavement reinforcement are expected for thicker pavements, where tensile strains at the bottom of asphalt layers caused by traffic loads are lower.

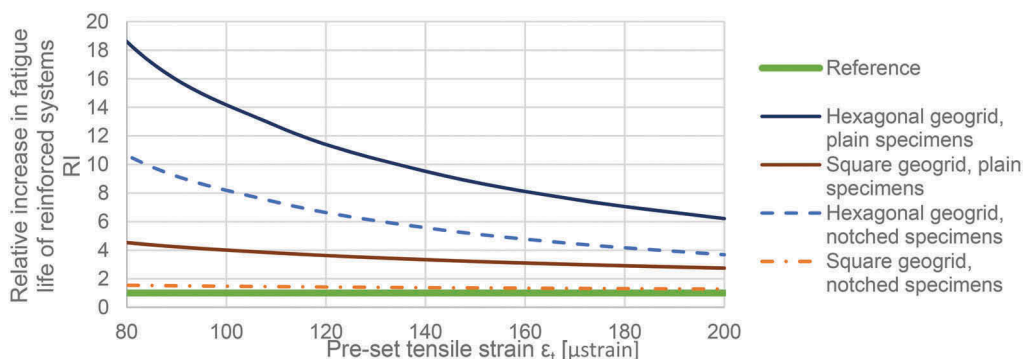


Figure 7. Relative increase in fatigue life of double-layered reinforced systems.

6 CONCLUSIONS

Analysis of the results of fatigue tests, which were performed on reference (unreinforced) systems and systems reinforced with geocomposites (both on plain and notched specimens), leads to the following conclusions:

- Strengthening the pavement structure with geocomposites increases both their load-bearing capacity and overall fatigue life.
- In the presented study, polypropylene stiff monolithic paving grids with integral junctions thermally bonded to polypropylene non-woven paving fabric were tested. For such geocomposites, the shape of the grid has an impact on fatigue life of the reinforced system. More beneficial effects are observed for hexagonal geogrids.
- The relative increase in fatigue life of the reinforced systems depends on the level of tensile strain at the bottom of the asphalt layers.
- More benefits in terms of pavement bearing capacity are expected in the case of reinforcement of thick, new asphalt pavements, where tensile strains at the bottom of the asphalt layers are lower and fatigue cracks have not been initiated yet.
- Using reinforcement in pavement structure postpones cracks formation in the upper layers.



- When using geocomposite reinforcement (i.e. geogrid bonded to paving fabric) one should expect that overall stiffness can be slightly reduced, as a consequence of slight differential movement between asphalt layers and geocomposite.
- Introducing geocomposite reinforcement between asphalt layers can also affect shear strength of interlayer bonding, but this should not have detrimental effect on overall pavement performance.

Future theoretical studies should be focused on solving the uncertainty in relationships between pre-set tensile strain in fatigue tests and tensile strain at the bottom of the asphalt layers in real pavement structure, as well as on the probable shift factor between results obtained from laboratory fatigue tests and fatigue life of pavements structures.

REFERENCES

- Al-Qadi, I. L. (2006). Pavement Interlayer System Mechanisms : Separation, Reinforcement, and Reflective Cracking Control. *Chinese Society of Pavement Engineering*, 73.
- Brown, S. F. (1985). Polymer grid reinforcement of asphalt. *Journal of Asphalt Paving Technology*, 54, 18–41.
- Canestrari, F., Belogi, L., Ferrotti, G., & Graziani, A. (2013). Shear and flexural characterization of grid-reinforced asphalt pavements and relation with field distress evolution. In *Materials and Structures*. <https://doi.org/10.1617/s11527-013-0207-1>
- Correia, N. de S. (2014). *Performance of flexible pavements enhanced using geogrid- reinforced asphalt overlays*. University of Sao Paulo, Brasil.
- Corté, J.-F., & Goux, M.-T. (1996). Design of pavement structures: the French technical guide. *Transportation Research Record*, 1539, 116–124. <https://doi.org/10.3141/1539-16>
- Graziani, A., Bocci, E., & Canestrari, F. (2014). Bulk and shear characterization of bituminous mixtures in the linear viscoelastic domain. *Mechanics of Time-Dependent Materials*. <https://doi.org/10.1007/s11043-014-9240-x>
- Jaskula, P., Rys, D., Stienss, M., Szydłowski, C., Golas, M., & Kawalec, J. (2021). Fatigue Performance of Double-Layered Asphalt Concrete Beams Reinforced with New Type of Geocomposites. *Materials*, 14(9), 2190. <https://doi.org/10.3390/ma14092190>
- Judycki, J., Jaskuła, P., Pszczoła, M., Ryś, D., Jaczewski, M., Alenowicz, J., Dołycki, B., & Stienss, M. (2017). New polish catalogue of typical flexible and semi-rigid pavements. *MATEC Web of Conferences*, 122. <https://doi.org/10.1051/mateconf/201712204002>
- Nguyen, M. L., Hornych, P., Le, X. Q., Dauvergne, M., Lumière, L., Chazallon, C., Sahli, M., Mouhoubi, S., Doligez, D., & Godard, E. (2021). Development of a rational design procedure based on fatigue characterisation and environmental evaluations of asphalt pavement reinforced with glass fibre grid. *Road Materials and Pavement Design*, 22(S1), S672–S689. <https://doi.org/10.1080/14680629.2021.1906304>
- Pasquini, E., Bocci, M., Ferrotti, G., & Canestrari, F. (2013). Laboratory characterisation and field validation of geogrid-reinforced asphalt pavements. *Road Materials and Pavement Design*, 14(1), 37–41. <https://doi.org/10.1080/14680629.2012.735797>
- Pszczola, M. (2019). Equivalent temperature for design of asphalt pavements in Poland. *MATEC Web of Conferences*, 262, 05010. <https://doi.org/10.1051/mateconf/201926205010>
- Ragni, D., Montillo, T., Marradi, A., & Canestrari, F. (2020). Fast falling weight accelerated pavement testing and laboratory analysis of asphalt pavements reinforced with geocomposites. *Lecture Notes in Civil Engineering*, 48(May), 417–430. https://doi.org/10.1007/978-3-030-29779-4_41
- Shukla, S. K., & Yin, J.-H. H. (2004). Functions and Installation of Paving Geosynthetics. *3rd Asian Regional Conference on Geosynthetics*, 314–321.
- Solatiyan, E., Bueche, N., & Carter, A. (2020). A review on mechanical behavior and design considerations for reinforced-rehabilitated bituminous pavements. *Construction and Building Materials*, 257, 119483. <https://doi.org/10.1016/j.conbuildmat.2020.119483>
- Spadoni, S., Ingrassia, L. P., Paoloni, G., Virgili, A., & Canestrari, F. (2021). Influence of Geocomposite Properties on the Crack Propagation and Interlayer Bonding of Asphalt Pavements. *Materials*, 14(5310), 1–18.
- Zieliński, P. (2013). Investigations of Fatigue of Asphalt Layers with Geosynthetics. *Archives of Civil Engineering*, 59(2). <https://doi.org/10.2478/ace-2013-0013>

